

# Optimal Transmit Antenna Deployment and Power Allocation for Wireless Power Supply in an Indoor Space

Kenneth MacSporran Mayer, *Student Member, IEEE*,

Laura Cottatellucci, *Member, IEEE*, and Robert Schober, *Fellow, IEEE*

## Abstract

As Internet of Things (IoT) devices proliferate, sustainable methods for powering them are becoming indispensable. The wireless provision of power enables battery-free operation and is crucial for complying with weight and size restrictions. For the energy harvesting components of these devices to be small, a high operating frequency is necessary. In conjunction with an electrically large antenna, the receivers may be located in the radiating near-field (Fresnel) region, e.g., in indoor scenarios. In this paper, we propose a wireless power transfer system to ensure a reliable supply of power to an arbitrary number of mobile, low-power, and single-antenna receivers, which are located in a three-dimensional cuboid room. To this end, we formulate a max-min optimisation problem to determine the optimal allocation of transmit power among an infinite number of radiating elements of the system's transmit antenna array. Thereby, the optimal deployment, i.e., the set of transmit antenna positions that are allocated non-zero transmit power according to the optimal allocation, is obtained implicitly. Generally, the set of transmit antenna positions corresponding to the optimal deployment has Lebesgue measure zero and the closure of the set has empty interior. Moreover, for a one-dimensional transmit antenna array, the set of transmit antenna positions is proven to be finite. The proposed optimal solution is validated through simulation. Simulation results indicate that the optimal deployment requires a finite number of transmit antennas and depends on the geometry of the environment and the dimensionality of the transmit antenna array. The robustness of the solution, which is obtained under a line-of-sight (LoS) assumption between the transmitter and receiver, is assessed in an isotropic scattering environment containing a strong LoS component.

## Index Terms

Near-field wireless power transfer, optimisation, Internet of Things.

K. M. Mayer, L. Cottatellucci and R. Schober are with the Institute for Digital Communications, Department of Electrical Engineering, Friedrich-Alexander University Erlangen-Nuremberg, Germany.

This work was (partly) funded by the Deutsche Forschungsgemeinschaft (DFG, German Research Foundation) – SFB 1483 – Project-ID 442419336, EmpkinS.

## I. INTRODUCTION

The number of Internet of Things (IoT) devices continues to grow rapidly and is expected to exceed 43 billion devices globally by 2023 [1]. Among those are wearable IoT devices, which are primarily intended for collecting data, e.g., for patient monitoring, treatment or rehabilitation [2], [3]. Wearable IoT devices are limited in terms of their weight and size and have to satisfy aesthetic requirements [4]. For example, these smart devices are not only designed as wearable accessories, but also as implants or tattoos and they may be embedded into textiles [2], [3]. As a consequence of the design requirements, wearable IoT devices rely on the interaction with a range of other devices, such as smartphones, for computing and communicating the collected information [2], [3].

Sustainability is a central theme for designing next-generation IoT technology and includes powering IoT devices, such as wearable systems, health monitoring systems, and implants, sustainably [1]. Currently, batteries are considered a hindrance in IoT technology due to the restrictions they impose on devices in terms of, e.g., size, weight, cost, and the need for replacement [1], [5], [6]. Alternative technologies, such as wireless power transfer (WPT) and energy harvesting (EH), facilitate the operation of battery-free IoT devices [1], [5], [6]. A reliable supply of power to IoT devices is ensured through available ambient power sources, such as ambient light, and dedicated power sources [1], [5]. Ambient sources can not ensure IoT devices are powered reliably as they are often uncontrollable. In contrast, dedicated power sources, such as dedicated electromagnetic (EM) radiation, offer controllability and thus, can secure powering IoT devices adequately [5].

High-frequency systems are attractive for short-range applications, such as indoor WPT [7]. The short wavelength allows the EH antenna of a device to be small [6]. For example, when utilising mmWave frequency bands, mm-scale antennas can be employed [6]. Consequently, the overall size of the devices can be reduced, allowing them to be less obtrusive and easier to integrate, e.g., into fabrics and textiles [1], [5]. Beyond that, a high carrier frequency in conjunction with electrically large antenna arrays leads to a significant increase in the radiating near-field (Fresnel) region. Although the Fresnel region could typically be neglected in conventional wireless systems, it has to be considered in, e.g., indoor scenarios, for high-frequency systems. Within the Fresnel region, the spherical nature of the EM wavefronts is non-negligible. Adequately capturing the EM wave characteristics in the Fresnel region demands modelling the wireless channel according to the spherical wavefront model (SWM), as the approximation by the planar wavefront model (PWM), typically utilised in the far-field region, does not hold

[8]–[10].

A WPT system operating in the Fresnel region is capable of focusing energy beams directly towards the receivers [7]. However, directing energy beams towards a multitude of possibly mobile receivers requires knowledge of their location, which is challenging and results in a highly complex communication system [1]. Especially, when devices are not intended to (continuously) broadcast their location, focusing energy beams towards them is not possible due to the missing location information. This holds true for wearable IoT devices, which often lack these communication capabilities [2], [3]. Consequently, there is a significant risk that the energy beams are misdirected and fail to reach the receivers, leading to an insufficient supply of power to these devices.

Considering the rapidly increasing number of IoT devices requiring a reliable supply of power [1]–[3], the development of a WPT system, capable of supplying them with power is an important and timely challenge. To ensure the reliable provision of power to an arbitrary number of devices in an environment, the WPT system must be capable of supplying the served environment with a minimum guaranteed level of power at any location. Thereby, a ubiquitous supply of power is offered in the considered environment.

In this paper, we propose a multi-user multiple-input single-output (MU-MISO) WPT system, which supplies an entire indoor space with a minimum level of guaranteed power. The transmitter of the WPT system employs a large transmit antenna array, which is mounted in the ceiling of a three-dimensional cuboid room, and comprises a continuum of infinitesimally small radiating elements. The WPT system can accommodate an arbitrary number of single-antenna receivers, located at arbitrary positions within the room. Assuming free space line-of-sight (LoS) propagation of the spherical EM wavefronts, we formulate an optimisation problem based on the distance information contained in the amplitude variations of the wireless links between every possible transmitter and receiver position to determine the optimal allocation of power among the transmit antennas. The optimal power allocated to transmit antennas can be zero and the optimisation problem for power allocation implicitly yields the optimal transmit antenna deployment. Specifically, it is optimal to deploy a transmit antenna where the optimal distribution of transmit power is non-zero. Hereby, the objective is to maximise the received power at the worst possible receiver positions in the indoor space. Thus, the proposed solution ensures a reliable supply of power to the receivers, which is a relevant criterion when there is no prior knowledge on the receivers' locations in the room. The main contributions of this paper can be summarised as follows:

- We formulate an optimisation problem to determine the optimal allocation of a finite amount of transmit power among an infinite number of radiating elements of a transmitter.
- Our analysis reveals that the support of the optimal allocation of transmit power is a set, whose closure has empty interior and Lebesgue measure zero. This holds for a set of isolated points. However, more complex structures that do not consume any measurable area could in theory also be contained in the set. The support of the optimal allocation corresponds to the optimal positions where transmit antennas should be deployed. In case the transmit antenna array is constrained to be one-dimensional, a stronger statement is possible and the optimal number of radiating elements is shown to be finite.
- Through simulation we show that the optimal number of transmit antennas is finite for one-dimensional and two-dimensional transmit antenna arrays. The actual number of antennas needed depends on the geometry of the environment. In the investigated environments, the optimal number is found to be surprisingly low.
- To validate our findings, the performance of the proposed optimal solution is evaluated against other power allocation schemes. For example, we investigate the loss in performance when removing the transmit antennas from the optimal transmit antenna array that operate with a small amount of transmit power. Additionally, the robustness of the proposed solution is investigated by adding small-scale fading to the LoS link.

The paper is organised in the following manner. In Section II, the system model is introduced. In Section III, the proposed optimisation problem is formulated and the structure of the optimal allocation of power is determined. As a result of Section III, we conjecture that the optimal solution of the optimisation problem is obtained by discretising the problem, and subsequently, solving it numerically; this is done in Section IV. In Section V, we provide a performance and sensitivity analysis of our approach, and Section VI concludes this paper.

## II. SYSTEM MODEL

The communication system considered in this paper consists of a transmit antenna array and an arbitrary number of single-antenna receivers. Throughout this paper, the terms "transmit antenna" and "radiating element" are used synonymously. An illustration of the considered system is given in Fig. 1, where the transmit antenna array is incorporated in the ceiling of a room.

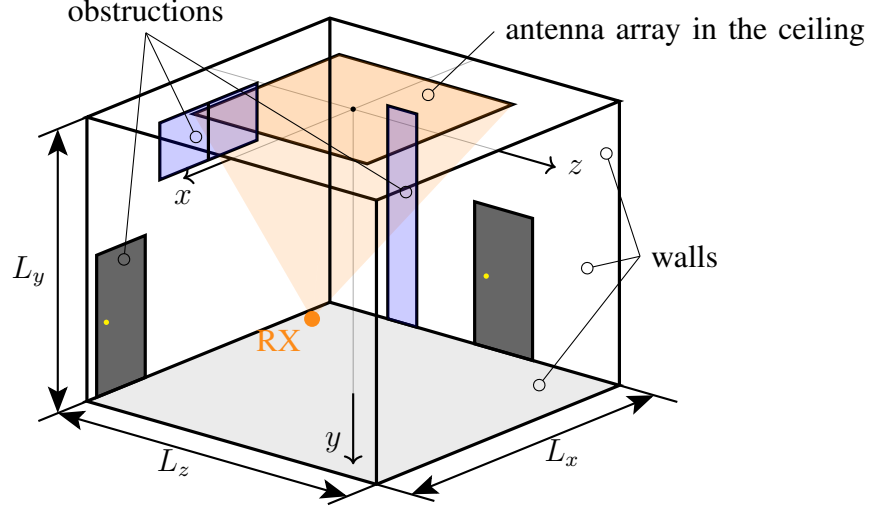


Fig. 1: Overview of the three-dimensional environment with a two-dimensional transmit antenna array consisting of a continuum of infinitesimally small antenna elements located in a subsection of the  $x$ - $z$  plane (orange). The LoS connections of the transmit antenna elements to one receiver (RX) are indicated in orange.

#### A. Environment

The environment considered in this paper is a three-dimensional cuboid room, where  $L_x$ ,  $L_y$ , and  $L_z$  define the size of the environment (see Fig. 1). The receivers, e.g., sensors or wearable devices, have to be supplied with power wirelessly and can be located anywhere inside the room. We define a receiver location as a small surface from which a receiver is capable of harvesting energy. The area of this surface is defined as  $\lambda^2/4$ , where  $\lambda$  is the wavelength. In this paper, we assume the transmit antenna array is located on the ceiling. The  $y$ -component of the room (see Fig. 1) is defined as the following closed interval in the set of real numbers  $\mathbb{R}$

$$\mathcal{Y} = \left\{ y \mid 0 \leq y \leq L_y, L_y > 0 \right\}. \quad (1)$$

The transmit antenna array is located at  $y = 0$  and is defined in Section II-B. At any other height level in the room, i.e.,  $y > 0$ , there exists a plane  $\mathcal{X} \times \mathcal{Z}$  which is partitioned into the disjoint elements from which a receiver can harvest energy. Thus, a receiver location is defined as the triplet  $(x_i, y, z_i) \in \mathcal{X} \times \mathcal{Y} \times \mathcal{Z}$  which corresponds to the  $i$ -th surface element of  $\mathcal{X} \times \mathcal{Z}$  at height  $y$ . For better legibility, the index  $i$  is dropped and a receiver location is written as  $(x, y, z) \in \mathcal{X} \times \mathcal{Y} \times \mathcal{Z}$ . The origin of the coordinate system is located in the middle of the ceiling of the room. Consequently,  $\mathcal{X}$  and  $\mathcal{Z}$  are bounded by  $\pm L_x/2$  and  $\pm L_z/2$ , respectively.

### B. Transmit Antenna Model

Although leveraging the full potential of a flexible transmit antenna placement would yield the best performance, the transmit antenna locations may be impractical or even infeasible in practice. Primarily, we consider a two-dimensional transmit antenna array. Additionally, we investigate the problem for a one-dimensional transmit antenna array which may be preferable in case of obstructions in the area of deployment.

The two-dimensional transmit antenna array is deployed on the ceiling, i.e., located on the plane  $y = 0$ , and is defined as the continuous surface  $\mathcal{X}_a \times \mathcal{Z}_a$  comprising infinitely many infinitesimally small antennas with

$$\mathcal{X}_a = \left\{ a_x \mid -L_{a_x}/2 \leq a_x \leq L_{a_x}/2, 0 < L_{a_x} \leq L_x \right\}, \quad (2)$$

and

$$\mathcal{Z}_a = \left\{ a_z \mid -L_{a_z}/2 \leq a_z \leq L_{a_z}/2, 0 < L_{a_z} \leq L_z \right\}. \quad (3)$$

Note that the plane  $\mathcal{X}_a \times \mathcal{Z}_a$  at  $y = 0$  is continuous whereas any  $\mathcal{X} \times \mathcal{Z}$  at  $y > 0$  is discrete. By assuming a continuous transmit antenna array, no constraint on the minimum size of a radiating element is imposed. The location of an infinitesimally small antenna is defined by the pair

$$(a_x, a_z) \in \mathcal{X}_a \times \mathcal{Z}_a. \quad (4)$$

Moreover, we assume that the surface, where the antenna array is located, i.e.,  $\mathcal{X}_a \times \mathcal{Z}_a$ , is free of obstructions. The radiating elements of the transmit antenna array are modelled as identical, omnidirectional antennas. As a special case of this transmit antenna array model, we also consider a one-dimensional transmit antenna array  $\mathcal{L}_a$  with an arbitrary direction in the plane at  $y = 0$ , where the location of a point source is defined as

$$a_l \in \mathcal{L}_a. \quad (5)$$

We neglect the impact of reactive near-field effects, such as mutual coupling, among the transmit antennas. This is justified by the fact that the optimal deployment is shown to require only a finite number of transmit antennas, which are spaced sufficiently far apart, see Section V-A. Thus, by virtue of the optimal solution's structure, we neglect the impact of mutual coupling.

*Remark 1:* Our optimal design constrained to the deployment of the transmit antennas on the ceiling of the room, i.e., at  $y = 0$ , can immediately be reformulated to the case where the transmit antenna array is integrated as part of a wall by exchanging the role of the  $y$ -component with the  $x$ -component or the  $z$ -component. As discussed in Section II-A, the planes parallel to

the antenna array need to be discretised into small surface elements where the receivers are able to harvest energy.

### C. Channel Model

In this paper, we consider two channel models, namely a LoS channel discussed in Section II-C1, and a Rician fading channel described in Section II-C2. The problem and the proposed solution approach presented in Section III are developed under LoS conditions based on the channel model in Section II-C1. This assumption on the channel model allows establishing an intuitive connection between the maximisation of the received power and the geometry underlying the problem. The robustness of the optimal solution is investigated through simulation in Section V, by assuming an isotropic scattering environment in the half-space in front of the transmit antenna array in addition to a strong LoS component, based on the Rician fading channel model in Section II-C2.

1) *LoS Channel*: The Fresnel region of a wireless system is characterised through the relationship between the wavelength of the EM waves, the size of the transmit antenna array, and the distance between the transmitter and the receiver. Specifically, a receiver is located within the Fresnel region if the distance between the receiver and the transmitter lies between the Fresnel distance  $d_{\text{Fresnel}} = \sqrt[3]{L^4/8\lambda}$  and the Fraunhofer distance  $d_{\text{Fraunhofer}} = 2L^2/\lambda$ , with  $L$  and  $\lambda$  being the largest dimension of the transmit antenna array and the wavelength, respectively [11]. The volume of the Fresnel region grows with increasing carrier frequency. In conventional wireless systems, the Fresnel region is negligibly small, however, when utilising mmWave frequency bands or higher, the size of the Fresnel region becomes significant, e.g., for indoor scenarios. Additionally, for very high carrier frequencies, such as in the mmWave or THz frequency bands, the reflection and scattering losses are severe, causing the LoS component to be dominant in the wireless channel [8], [12]. Thus, a LoS channel is typically assumed for wireless systems operating in the Fresnel region [7], [11], [13]. We note that interruptions of the LoS due to obstructions cause blockages [7] and we reduce the risk of channel blockage by placing the transmit antenna array on the ceiling of the room instead of on one of the walls (see Section II-B). For the analytical tractability of the system design, we make the assumption that a LoS connection between the transmit antennas and the receiver exists and do not consider the impact of channel blockages in this paper.

Under free-space LoS conditions, the equivalent complex baseband channel between the

transmit antenna element at  $(a_x, a_z)$  and a receiver at  $(x, y, z)$  is given by [14]

$$g_{xyz}(a_x, a_z) = \frac{\sqrt{c}}{D_{xyz}(a_x, a_z)} e^{-j\frac{2\pi}{\lambda} D_{xyz}(a_x, a_z)}, \quad (6)$$

where  $D_{xyz}(a_x, a_z)$  is the distance between the antenna element at  $(a_x, a_z)$  and a receiver at  $(x, y, z)$ , i.e.,  $D_{xyz}(a_x, a_z) = \sqrt{(x - a_x)^2 + y^2 + (z - a_z)^2}$  and  $c$  is the channel power gain at the reference distance of 1 meter. By virtue of the spherical nature of the EM wavefronts, both the amplitude and the phase of  $g_{xyz}(a_x, a_z)$  depend on distance  $D_{xyz}(a_x, a_z)$ . In contrast, when the EM wavefronts are modelled as planar waves (far-field approximation), the *path loss* between all transmit antenna elements and a receiver is assumed to be constant, i.e.,  $D_{xyz}(a_x, a_z) \approx D_{xyz}$ , where  $D_{xyz}$  is constant.

2) *Rician Fading Channel*: While the assumption of a strong LoS channel is valid for very high carrier frequencies, there may still be a low-power small-scale fading component. This requires including a non-line-of-sight (NLoS) component in the wireless channel model [14]. An appropriate statistical model, under isotropic scattering, for the NLoS channel is given by spatially correlated Rayleigh fading [15], [16], [17]. Together, the NLoS and LoS components constitute a Rician fading channel.

The problem considered in this paper is formulated for the LoS channel model. The robustness of the solution is verified using a Rician channel model, which is defined in Section V-C.

#### D. Transmit Signal Model

The amount of power harvested by a device is a monotonically increasing function of the received signal power [18]. Moreover, the received signal power depends on the transmitted signal. The transmit signal  $t(a_x, a_z)$  emitted by the transmit antenna located at  $(a_x, a_z)$  is given by

$$t(a_x, a_z) = \sqrt{p(a_x, a_z)} e^{j\theta(a_x, a_z)}, \quad (7)$$

where  $p(a_x, a_z) \geq 0$  is the non-negative transmit power and  $\theta(a_x, a_z)$  is the phase. Since there is no information on the location of the receivers, the transmit signal should illuminate the entire environment. Therefore, the phases are assumed to be independent and identically distributed (i.i.d.) among the transmit antennas. Consequently, the received signal at receiver position  $(x, y, z)$  is given by

$$r_{xyz} = \iint_{\mathcal{X}_a \times \mathcal{Z}_a} t(a_x, a_z) g_{xyz}(a_x, a_z) da_x da_z + n \quad (8)$$



where  $n$  is additive white Gaussian noise with zero mean and variance  $\sigma_n^2$ , i.e.,  $n \sim \mathcal{CN}(0, \sigma_n^2)$ .

The power of the received signal is given by

$$\gamma_{xyz} = \mathbb{E}_P \left\{ \left| \iint_{\mathcal{X}_a \times \mathcal{Z}_a} t(a_x, a_z) g_{xyz}(a_x, a_z) da_x da_z \right|^2 \right\} = c \iint_{\mathcal{X}_a \times \mathcal{Z}_a} \frac{p(a_x, a_z)}{[D_{xyz}(a_x, a_z)]^2} da_x da_z, \quad (9)$$

where  $\mathbb{E}_P\{\cdot\}$  is the expectation operator with respect to (w.r.t.) the distribution  $P$ , which is defined as

$$dP(a_x, a_z) = p(a_x, a_z) da_x da_z. \quad (10)$$

Therefore, the received power is directly proportional to

$$\iint_{\mathcal{X}_a \times \mathcal{Z}_a} f_{xyz}(a_x, a_z) dP(a_x, a_z), \quad (11)$$

with

$$f_{xyz}(a_x, a_z) = \left( \frac{1}{D_{xyz}(a_x, a_z)} \right)^2. \quad (12)$$

The overall amount of transmit power is constrained to be finite, i.e.,

$$\iint_{\mathcal{X}_a \times \mathcal{Z}_a} p(a_x, a_z) da_x da_z = \iint_{\mathcal{X}_a \times \mathcal{Z}_a} dP(a_x, a_z) = 1, \quad (13)$$

where, without loss of generality, the transmit power is normalised to unity. Note that the normalised distribution of power can be interpreted as a probability distribution.

### III. OPTIMAL POWER ALLOCATION

Our goal is to supply an undefined number of receivers with power anywhere in the environment. This objective can be achieved by maximising the received signal power for the worst possible receiver position(s) in the environment, which leads to a max-min optimisation problem. In this section, we formulate this optimisation problem to determine the optimal allocation of transmit power among the radiating elements of the transmitter. This optimal allocation provides the optimal positions for the deployment of transmit antennas as a byproduct. Namely, it is optimal to deploy a transmit antenna at any point  $(a_x, a_z)$  where the optimal distribution of transmit power is non-zero.

### A. Problem Formulation

Maximising the received power at location  $(x, y, z)$  in the environment is achieved by maximising the expectation of function  $f_{xyz}$  i.e.,  $E_P\{f_{xyz}\}$ , defined in (11), via an optimal allocation of the transmit powers among the transmit antennas, where  $P$  is an element of the set of distributions  $\Omega$ , i.e.,  $P \in \Omega$ . Hereby, the non-negativity and finite power constraints, which have been introduced in Section II-B, apply to every element of  $\Omega$ . Moreover, the function  $P(a_x, a_z)$  is restricted to the set  $\mathcal{X}_a \times \mathcal{Z}_a$ , and as a consequence of (13),  $P(a_x, a_z)$  is bounded by one and thus, square-integrable. Therefore, the set of considered distributions  $\Omega$  is a subset of the square-integrable (finite energy) functions defined over the transmit antenna domain and denoted as  $\mathcal{L}^2(\mathcal{X}_a \times \mathcal{Z}_a)$ , i.e.,  $P(a_x, a_z) \in \Omega \subset \mathcal{L}^2(\mathcal{X}_a \times \mathcal{Z}_a)$ . The set  $\Omega$  is further characterised through the following lemma.

**Lemma 1.** *The set of distributions  $\Omega \subset \mathcal{L}^2(\mathcal{X}_a \times \mathcal{Z}_a)$  is a weakly compact space in the weak topology and convex.*

*Proof:* The proof is found in Appendix A. ■

Ensuring that receivers are supplied with power anywhere in the environment is achieved by maximising the received signal power at the worst possible receiver position(s) in the environment. This can be formulated as the following max-min optimisation problem

$$\underset{P \in \Omega}{\text{maximise}} \quad \min_{\substack{(x,y,z) \\ \in \mathcal{X} \times \mathcal{Y} \times \mathcal{Z}}} E_P\{f_{xyz}\}. \quad (14)$$

The best worst-case performance, i.e., the optimal objective value of Problem (14), is denoted by  $m$  and is defined as

$$m = \min_{\substack{(x,y,z) \\ \in \mathcal{X} \times \mathcal{Y} \times \mathcal{Z}}} E_{P^*}\{f_{xyz}\}, \quad (15)$$

where  $P^*$  is the optimal distribution of power. Note that Problem (14) is linear in  $P$ . The feasibility of Problem (14) is ensured through the compactness of  $\Omega$  shown in Lemma 1, i.e.,  $\Omega$  is closed and bounded.

### B. Critical Receiver Positions

By identifying the receiver locations, where the received signal power is the lowest, the complexity of solving Problem (14) can be reduced. These critical locations are defined w.r.t. the optimal distribution of power  $P^*$ . To this end, the set containing the critical receiver positions

when power is allocated optimally is denoted by  $\mathcal{R}_{\text{crit}}$ . The set of non-critical positions is the complement of  $\mathcal{R}_{\text{crit}}$ , i.e.,  $\mathcal{R}_{\text{crit}}^c$ . After the power has been optimally allocated among the transmit antenna elements, the amount of received signal power at a critical receiver position  $(x, y, z) \in \mathcal{R}_{\text{crit}}$  will be below the received signal power at any non-critical location  $(x, y, z) \in \mathcal{R}_{\text{crit}}^c$ . Next, the set of critical receiver positions is defined more precisely.

**Lemma 2.** *For any  $(x, z) \in \mathcal{X} \times \mathcal{Z}$ , the worst performance is attained at  $y = L_y$ . Consequently, all critical positions are located at  $y = L_y$ , i.e.,  $\mathcal{Y}_{\text{crit}} = \{L_y\}$ .*

*Proof:* Since  $f_{xyz}$  is a monotonically decreasing function of  $y$ , the lowest objective value is obtained in the plane with  $y = L_y$ . ■

Thus, the objective function in Problem (14) is defined based on functions  $f_{xz}(a_x, a_z) := f_{xyz}(a_x, a_z)|_{y=L_y}$ . Note that  $f_{xz}(a_x, a_z)$  is a bounded and square-integrable function. Problem (14) is equivalently reformulated in the following lemma.

**Lemma 3.** *Assume that the set of critical positions  $\mathcal{R}_{\text{crit}} \subseteq \mathcal{X} \times \mathcal{Y}_{\text{crit}} \times \mathcal{Z}$  is known. Then, solving Problem (14) is equivalent to solving the following problem*

$$\underset{o \in \mathbb{R}, P \in \Omega, \Lambda}{\text{maximise}} \quad \underbrace{o - \sum_{\mathcal{R}_{\text{crit}}} (o - \mathbb{E}_P\{f_{xz}\}) \lambda_{xz}}_{J(P)}, \quad (16)$$

where  $\Lambda$  is the set of positive variables  $\lambda_{xz} > 0, \forall (x, y, z) \in \mathcal{R}_{\text{crit}}$ . When allocating power optimally through  $P^*(a_x, a_z)$ , the optimal objective value is  $o^* = m$  and the following conditions should also hold

$$[(\lambda_{xz} > 0 \implies m = \mathbb{E}_{P^*}\{f_{xz}\}) \text{ or } (m < \mathbb{E}_{P^*}\{f_{xz}\} \implies \lambda_{xz} = 0)], \forall (x, y, z) \in \mathcal{X} \times \mathcal{Y}_{\text{crit}} \times \mathcal{Z}. \quad (17)$$

*Proof:* The proof is presented in Appendix B. ■

The objective function in Problem (16) is referred to as  $J(P)$  in the following. Note that Problem (16) is a convex optimisation problem, which is readily apparent when the problem is stated in epigraph form [19] (see Appendix B).

### C. Optimal Structure of Power Distribution

In this section, we establish a relation between Problem (16) and the problem of finding the optimal amplitude-constrained input distribution for reaching the information capacity of Gaussian channels studied in [20]–[22]. In [20] and [21], the authors determine the optimal

input distribution of transmit symbols, which are bounded in amplitude, for achieving information capacity, whereas our problem lies in identifying the optimal allocation of transmit powers, under geometrical constraints regarding the transmit antenna array. Beyond communication problems [20], similar results on the optimal input distribution in WPT applications have been established in [21]. First, we consider the optimisation of a two-dimensional distribution  $P(a_x, a_z)$  which is significantly different to the problems involving one-dimensional distributions such as [20] and [21]. Specifically, the properties of the optimal distribution's structure are less stringent. The analysis of optimisation problems involving input distributions with a dimensionality greater than one has been studied in [22]. Subsequently, we consider the optimisation problem with a one-dimensional distribution, which allows characterising the optimal distribution as in [20] and [21].

In the following, we investigate properties, which apply to the optimal distribution of power and allow to characterise the optimal set of transmit antenna positions. The main results are stated in Propositions 2 and 3 for the optimal distribution of power over a two-dimensional surface and in Proposition 4 for the optimal one-dimensional distribution. First, a necessary and sufficient condition for the optimal distribution of power  $P^*$  is established in Proposition 1 and Corollary 1.

**Proposition 1.** *Consider the optimisation problem in (16). There exists an optimal distribution of power  $P^*(a_x, a_z)$  which attains the maximum  $m$  of Problem (16) if and only if the following condition holds*

$$\iint_{\mathcal{X}_a \times \mathcal{Z}_a} \bar{f}(a_x, a_z) \, dP(a_x, a_z) \leq m, \quad \forall P \in \Omega, \quad (18)$$

where  $\bar{f}(a_x, a_z)$  is given by

$$\bar{f}(a_x, a_z) = \frac{\sum_{\mathcal{R}^{\text{crit}}} f_{xz}(a_x, a_z) \lambda_{xz}}{\sum_{\mathcal{R}^{\text{crit}}} \lambda_{xz}}, \quad (19)$$

and (18) is satisfied with equality for the optimal distribution of power  $P^*(a_x, a_z)$ .

*Proof:* This proposition is proven in Appendix C ■

Intuitively, function  $\bar{f}$  can be interpreted as the weighted average of  $f_{xz}$  over the receiver positions  $\mathcal{X} \times \mathcal{Z}$  at  $y = L_y$ . The weights are given by the variables  $\lambda_{xz} / \sum_{\mathcal{R}^{\text{crit}}} \lambda_{xz}$  and thus, only critical receiver positions contribute to  $\bar{f}$ . Note that the optimal distribution  $P^*$  is not necessarily unique since  $J(P)$  is linear in  $P$  and not strictly concave as in the problems considered in [20], [21]. Additionally, Proposition 1 provides a condition for the existence of  $P^*$ . Obtaining  $P^*$  requires determining the variables  $\lambda_{xz}$  satisfying (18) and (19).

Next, the optimality condition for  $P^*$ , given in Proposition 1, is restated in a more intuitive manner. This requires defining the support of  $P^*$ , which is analogous to the definition in [22]. A transmit antenna position  $(a_x, a_z)$  is called a *point of increase* of the optimal distribution  $P^*$  if for any open subset  $O \subset \mathbb{R}^2$  containing  $(a_x, a_z)$ ,  $P^*(O) > 0$  holds [22]. The set of points of increase of  $P^*$  is defined as  $\mathcal{E}(P^*) \subseteq \mathbb{R}^2$ . Note that  $P^*(\mathcal{E}(P^*)) = 1$  [22]. Moreover,  $\mathcal{E}(P^*)$  is the smallest closed subset of  $\mathbb{R}^2$  such that  $P^*(\mathcal{E}(P^*)) = 1$  [22]. Note that  $P \in \Omega$  is restricted to  $\mathcal{X}_a \times \mathcal{Z}_a \subset \mathbb{R}^2$  and thus,  $\mathcal{E}(P^*) \subseteq \mathcal{X}_a \times \mathcal{Z}_a$ . We define  $\mathcal{E}(P^*)$  as the support of  $P^*$ .

**Corollary 1.** *Consider the optimisation problem in (16). There exists an optimal distribution of power  $P^*$  for Problem (16) if and only if  $\bar{f}(a_x, a_z)$  satisfies the following equations*

$$\bar{f}(a_x, a_z) \leq m, \quad \forall (a_x, a_z) \in \mathcal{X}_a \times \mathcal{Z}_a, \quad (20)$$

$$\bar{f}(a_x, a_z) = m, \quad \forall (a_x, a_z) \in \mathcal{E}(P^*). \quad (21)$$

*Proof:* The proof is provided in Appendix D. ■

Thus, Corollary 1 describes the relationship between the optimal distribution of transmit power  $P^*$  for attaining the optimal objective value  $m$  of Problem (16) and the optimal set of transmit antenna positions  $\mathcal{E}(P^*)$ , i.e., the support of  $P^*$ .

Based on the optimality conditions on  $P^*$  defined in Proposition 1 and Corollary 1, the set of optimal antenna positions is characterised more precisely. First, we complete our analysis of the two-dimensional distribution  $P^*(a_x, a_z)$ . Subsequently, we characterise the set of optimal transmit antenna positions under the constraint of a one-dimensional deployment.

**Proposition 2.** *The support  $\mathcal{E}(P^*) \subset \mathcal{X}_a \times \mathcal{Z}_a$  of the optimal two-dimensional distribution of power  $P^*$  is a nowhere dense set of  $\mathcal{X}_a \times \mathcal{Z}_a$ .*

*Proof:* The proof is provided in Appendix E. ■

**Proposition 3.** *The support  $\mathcal{E}(P^*) \subset \mathcal{X}_a \times \mathcal{Z}_a$  of the optimal two-dimensional distribution of power  $P^*$  is of Lebesgue measure zero.*

*Proof:* The proof is provided in Appendix F. ■

Thus,  $\mathcal{E}(P^*)$  is a set of pairs  $(a_x, a_z)$ , which define the optimal transmit antenna positions, that is nowhere dense and has Lebesgue measure zero, i.e., the set  $\mathcal{E}(P^*)$  does not occupy any measurable surface in  $\mathcal{X}_a \times \mathcal{Z}_a$ . Intuitively, the set  $\mathcal{E}(P^*)$  could consist of isolated points scattered throughout  $\mathcal{X}_a \times \mathcal{Z}_a$  since both properties hold in this case. On the other hand, Propositions 2

and 3 do not preclude the possibility of  $\mathcal{E}(P^*)$  containing more complex structures, such as continuous one-dimensional structures, as long as  $\mathcal{E}(P^*)$  is of nowhere dense and of measure zero. This is further investigated in Section IV. Moreover, observe that, by virtue of the max-min problem, the optimal distribution must be symmetrical w.r.t. the  $x$ -axis and the  $z$ -axis, i.e.,  $P^*(a_x, a_z) = P^*(-a_x, a_z) = P^*(-a_x, -a_z) = P^*(a_x, -a_z)$ . Violating this symmetry condition would lead to a decrease in performance at the worst possible receiver positions, which would decrease the objective value.

The results presented in this section, which allowed drawing conclusions regarding the optimal deployment of transmit antennas  $\mathcal{E}(P^*)$ , pertained to the analysis of a two-dimensional distribution of power. In the following, we restrict the antennas to lie on the one-dimensional set  $\mathcal{L}_a$ , which results in a problem analogous to [20], [21] (see Section II-B). Consequently, the optimal distribution of power  $\tilde{P}^*(a_l)$  along  $\mathcal{L}_a$  is one-dimensional. This problem is investigated in the following, whereby the set of optimal transmit antenna positions  $\tilde{\mathcal{E}}(\tilde{P}^*) \subset \mathcal{L}_a$  is shown to be finite.

**Proposition 4.** *The support  $\tilde{\mathcal{E}}(\tilde{P}^*) \subset \mathcal{L}_a$  of the optimal one-dimensional distribution is a finite set of points.*

*Proof:* The proof is provided in Appendix G. ■

#### IV. SYSTEM DISCRETISATION

In the following, the numerical analysis of the optimal deployment of the transmit antennas is studied. In order to solve Problem (14) numerically, the set of transmit antenna positions  $\mathcal{X}_a \times \mathcal{Z}_a$  and  $\mathcal{L}_a$  have to be discretised. For a one-dimensional transmit antenna array, we have proven in Proposition 4 that a finite number of transmit antennas placed in  $\tilde{\mathcal{E}}(\tilde{P}^*) \subset \mathcal{L}_a$  is optimal. For a two-dimensional transmit antenna array, Proposition 3 guarantees that the optimal deployment of transmit antennas is on a set  $\mathcal{E}(P^*) \subset \mathcal{X}_a \times \mathcal{Z}_a$  with Lebesgue measure zero. We conjecture that the optimal solution to Problem (14) is obtained through discretising the problem, and subsequently, solving it numerically. This assumption holds true if the solution of the optimisation problem remains unchanged for finer levels of discretisation (LoD), i.e., for an increasing granularity of the sampling grid. Further, we conjecture that the transmit antennas are given as a collection of isolated points scattered within  $\mathcal{X}_a \times \mathcal{Z}_a$  since Proposition 2 ensures that the optimal set of transmit antennas  $\mathcal{E}(P^*) \subset \mathcal{X}_a \times \mathcal{Z}_a$  is nowhere dense, in addition to having Lebesgue measure zero. Thereby, it is necessary to investigate whether the number of transmit

antennas increases monotonically for finer LoD or if the number of transmit antennas remains constant. Intuitively, if the latter is true, there is an optimal, finite number of transmit antennas, which depends on the geometrical properties of the environment, i.e.,  $L_x$ ,  $L_y$ , and  $L_z$ , at least from a practical point of view. The three-dimensional environments, which are investigated in this paper, are listed in Tab. I. The difference between the environments is the ratio of height

TABLE I: Definition of the four environments analysed in Sections IV and V.

Height $L_y$ in [m]	Width $L_x$ in [m]	Depth $L_z$ in [m]	$\frac{\text{Height}}{\text{Width}}$
2	2	2	1/1
2	6	6	1/3
2	8	8	1/4
2	10	10	1/5

to width since the width and depth of the room are chosen to be equal. The environments are denoted by their height-to-width ratio.

#### A. Discretised Optimisation Problem

In the following, the set of transmit antenna positions, i.e.,  $\mathcal{X}_a \times \mathcal{Z}_a$  for the two-dimensional problem and  $\mathcal{L}_a$  for the one-dimensional problem, is discretised. In this paper, we only investigate systems where the antenna array covers the entire ceiling, i.e.,  $L_{ax} = L_x$  and  $L_{az} = L_z$ . The one-dimensional antenna array is also placed on the ceiling along the  $x$ -axis, i.e.,  $\mathcal{L}_a = \mathcal{Z}_a$ . Moreover, we define  $L_x = L_z$ . The LoD is defined as the number  $N + 1$  of equally-sized intervals into which the sets  $\mathcal{X}_a$ ,  $\mathcal{Z}_a$ , and  $\mathcal{L}_a$  are partitioned, respectively. Consequently, we have a grid of antenna positions with  $(N + 1)^2$  elements in  $\mathcal{X}_a \times \mathcal{Z}_a$  and  $N + 1$  elements in  $\mathcal{L}_a$ , respectively. The position of transmit antenna  $i$ , which corresponds to one element of the grid, is given as  $(a_{ix}, a_{iz})$ , with  $i = 1, \dots, (N + 1)^2$ , in two dimensions and  $(a_{il})$ , with  $i = 1, \dots, N + 1$ , in one dimension. By utilising the definitions in Section II-D, Problem (14) is discretised as follows

$$\begin{aligned} & \underset{o \in \mathbb{R}, p(a_{ix}, a_{iz})}{\text{maximise}} && o \end{aligned} \tag{22a}$$

$$\begin{aligned} & \text{subject to} && o \leq \sum_{(a_{ix}, a_{iz})} f_{xz}(a_{ix}, a_{iz}) p(a_{ix}, a_{iz}), \quad \forall (x, y, z) \in \mathcal{X} \times \mathcal{Y}_{\text{crit}} \times \mathcal{Z}, \end{aligned} \tag{22b}$$

$$\sum_{(a_{ix}, a_{iz})} p(a_{ix}, a_{iz}) = 1, \tag{22c}$$

$$p(a_{ix}, a_{iz}) \geq 0, \tag{22d}$$

where the problem has been rewritten in epigraph form [19]. After discretisation, the convex optimisation problem in (22) can be solved efficiently, for example, by applying the interior-point method [19]. The problem is solved using standard numerical tools for convex optimisation, such as CVXPY [23], [24]. Any value below  $10^{-6}$  in the optimal distribution of power was deemed to be a numerical error and was set to zero. In the worst case, values below  $10^{-6}$  accounted for less than  $10^{-5}\%$  of the total power distributed among the transmit antennas.

### B. Level of Discretisation

There is an inherent trade-off between the computational complexity of solving a problem and the accuracy of its solution. The necessary LoD is determined based on a desired accuracy and a criterion to assess whether the proposed solution is sufficiently accurate. To this end, Problem (22) was solved repeatedly for increasing granularity of the sampling grid. Subsequently, the differences between the objective values of consecutive iterations were evaluated. Once the relative difference dropped below 0.1%, the LoD was deemed fine enough.

In Fig. 2, the relative difference between the objective values, i.e., the difference between the current and previous objective value divided by the current objective value, was calculated for every  $N$ . As the LoD increases, the accuracy increases for all investigated environments since the objective value stabilises. Moreover, for decreasing height-to-width ratios, larger variations among the objective values of consecutive iterations occur.

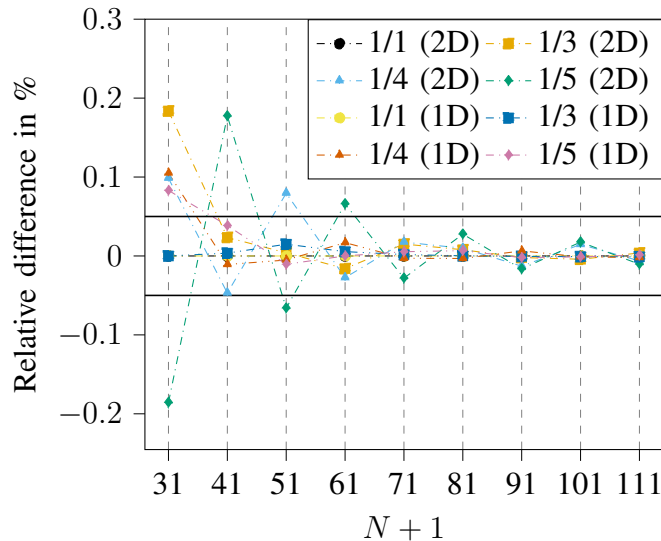


Fig. 2: Relative difference between objective values for increasing  $N$  for the environments defined in Tab. I. The black lines at  $\pm 0.05\%$  indicate the desired accuracy threshold of 0.1%.



### C. Finiteness of the Optimal Power Distribution

In this section, the optimal number of transmit antennas  $N_t^{*1}$  is investigated for an increasing LoD. To this end, the absolute number of optimal transmit antennas per environment is displayed in Fig. 3. In Fig. 3, one can observe that the optimal number of transmit antennas  $N_t^*$  does not

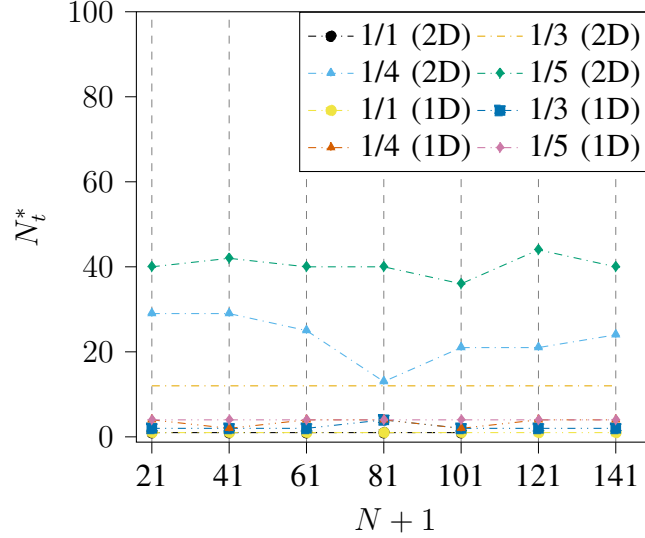


Fig. 3: Optimal number of transmit antennas, i.e., number of positions where non-zero powers are allocated by the optimal distribution, for increasing  $N$  for the environments given in Tab. I.

increase monotonically for different LoDs, which suggests that a finite number of antennas is optimal, even for a two-dimensional array. The optimal number of antennas to be deployed depends on the geometry of the environment and the dimensionality of the transmit antenna array. Moreover, one can assume that the optimal deployment of antennas can be embedded more efficiently in grids with a certain number of cells compared to others, depending on how well the optimal geometrical arrangement can be represented within the grid cells (see Section V-A). Consequently, slight fluctuations regarding the optimal number of transmit antennas are expected, which are visible in Fig. 3. However, note that these fluctuations are negligible compared to the difference in the number of grid cells among different LoDs, especially for the two-dimensional array with  $(N+1)^2$  cells.

In general, the optimal number of transmit antennas is larger when employing a two-dimensional antenna array compared to the deployment over a one-dimensional transmit antenna array.

<sup>1</sup>The optimal number of transmit antennas is defined as the number of non-zero values in the solution  $p^*(a_{ix}, a_{iz})$  of Problem (22).

Moreover, for a decreasing height-to-width ratio, the optimal number of transmit antennas increases, especially when employing a two-dimensional antenna array.

## V. PERFORMANCE AND SENSITIVITY ANALYSIS

Unless specified otherwise, all simulations in the following are performed at LoD  $N + 1 = 81$ .

### A. Heatmaps of Optimal Distributions

The solution  $p^*(a_{ix}, a_{iz})$  of Problem (22) is visualised in Fig. 4 using heatmaps for the different environments considered in Tab. I. The value zero is depicted using white colour, while the non-zeros are represented by a colour corresponding to the percentage of power allocated to the position. Thus, transmit antennas are represented by a colour different from white.

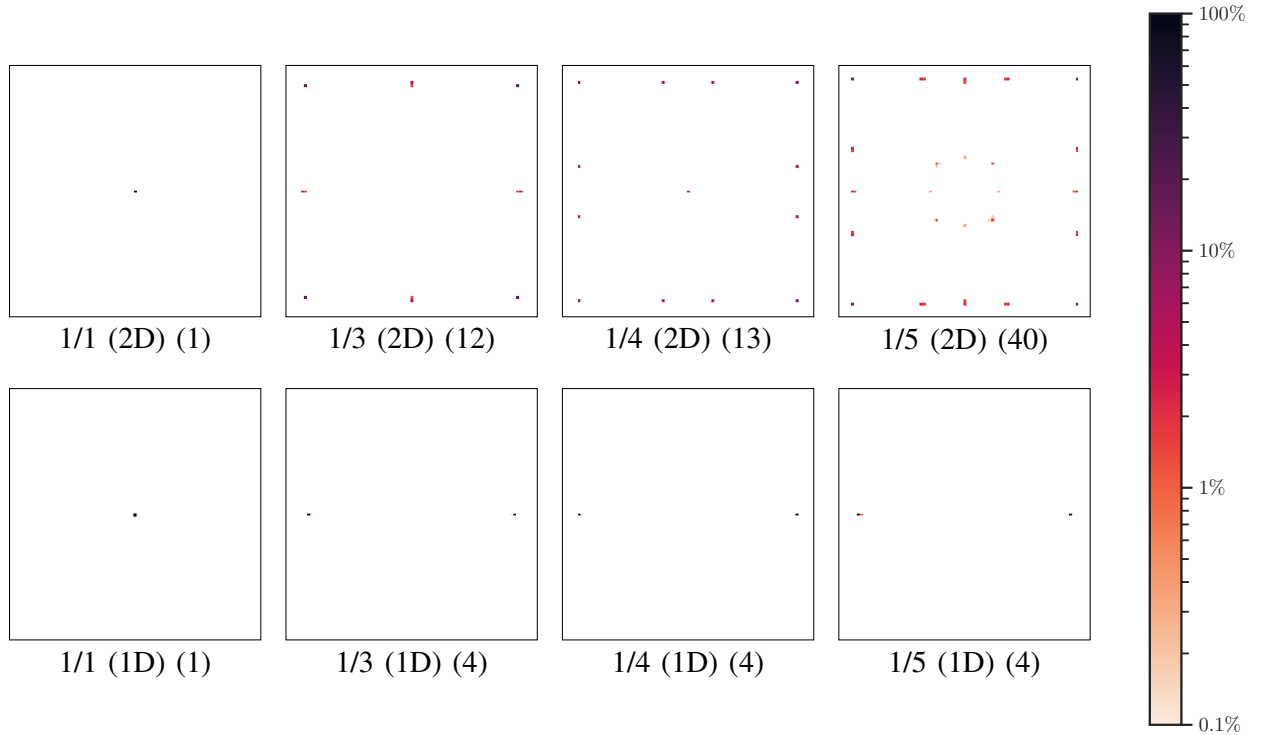


Fig. 4: Heatmaps of optimal power distributions for the environments listed in Tab. I with  $N + 1 = 81$ . Each subtitle indicates the geometry of the environment in Tab. I, the dimensionality of the transmit antenna array, and the number of non-zeros of  $p^*(a_{ix}, a_{iz})$  in brackets, i.e., the optimal number of transmit antennas. The relative amount of power allocated to an antenna is color-coded according to the colour bar on the right.

This depiction supports our conjecture that the optimal transmit antenna positions are isolated points. For a height-to-width ratio equal to one, it is optimal to place a single antenna in the centre of the ceiling. This is discussed further in the next section.

### B. Minimum Received Power and Comparison to Alternative Deployments

In this section, the performance of the proposed optimal two-dimensional distribution of power is measured in terms of the minimum received power in the environment. The proposed optimal method is denoted by M-OPT. Moreover, the performance is compared to other power allocation methods, which are listed below:

- Optimal deployment and power allocation for the far-field operating regime. The achievable performance gain of modelling the system in the Fresnel region is highlighted by comparing the proposed approach to the optimal power distribution designed for the far-field operating regime. Due to the constant path loss in the far-field, only a single transmit antenna is deployed and it is allocated all the available power. Moreover, the antenna is positioned at the centre of the ceiling as any other position would yield a worse objective value in the max-min problem. This benchmark scheme is referred to as M-FF.
- A uniform power distribution across the antenna array, where an antenna is located at every grid cell and the power is split equally among the antennas. This benchmark scheme is referred to as M-UNI.
- Suboptimal schemes obtained from the proposed optimal approach. Hereby, optimally deployed transmit antennas operating with low transmit power are removed, i.e., small non-zero values are set to zero in the distribution, and subsequently, the allocated powers are re-normalised for a fair comparison at equal total power. More specifically, the  $x$ -th percentile of the allocated power levels was calculated and transmit antennas operating at a power level lower than the one corresponding to the  $x$ -th percentile were removed, followed by the re-normalisation of power. We investigated the following 25th, 50th, 75th, and 90th percentiles of the non-zero values. The schemes are referred to as M-S25, M-S50, M-S75, M-S90, respectively.

The results are illustrated in Fig. 5 for environments with different geometries. The proposed optimal power distribution outperforms all other approaches. We assume a transmit power of 10W, a fixed height of 2m, and a wavelength of  $\lambda = 3 \cdot 10^{-3}$ m. The loss compared to the proposed optimal solution is calculated by dividing the objective value of a benchmark scheme or a suboptimal scheme by the objective value obtained through the optimal deployment and power allocation, i.e., the solution of Problem (22). For a fixed height, the size of the environment increases for decreasing height-to-width ratio. Consequently, the minimum received power decreases since the total transmit power is limited. For height-to-width ratios close to

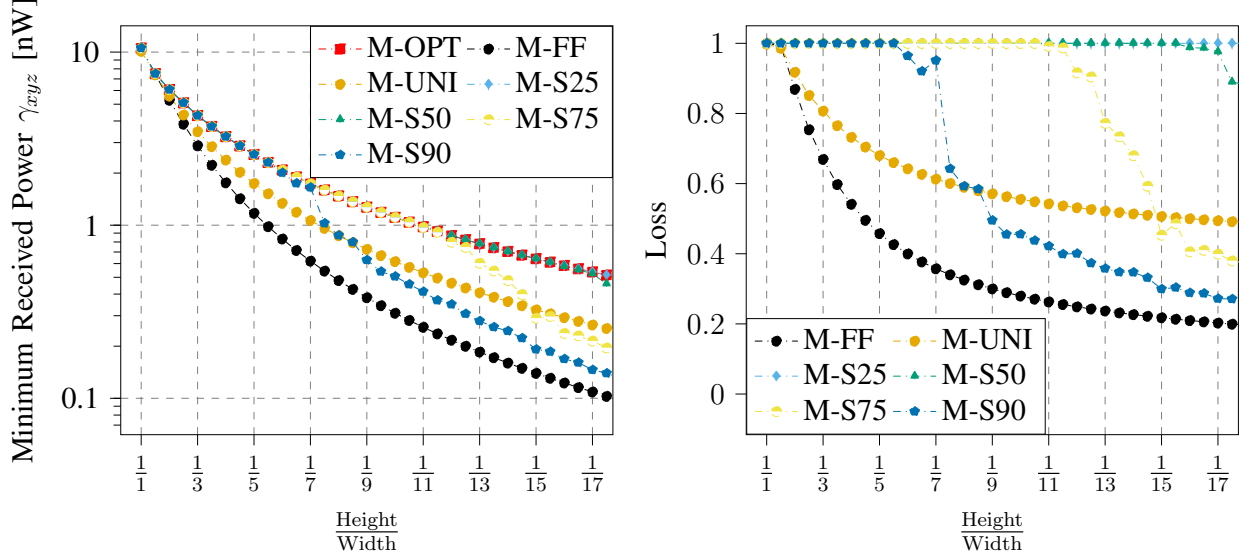


Fig. 5: Minimum received power at the worst location in the environment and loss of the benchmark schemes and suboptimal schemes compared to proposed optimal deployment and power allocation. The height is fixed at 2m.

one, the loss is small. However, the loss compared to the proposed optimal solution increases for decreasing height-to-width ratio. Note that the received power can be increased by adding more receive antennas. The largest loss occurs when utilising the optimal distribution for the far-field operating regime. If the height-to-width ratio is larger than or equal to one, the optimal solution coincides with M-FF. In this case, the proposed system does not have to be optimised for operating in the Fresnel region. Especially, for small height-to-width ratios, a uniform distribution of power across all antenna elements is also highly suboptimal.

The suboptimal schemes M-S25, M-S50, M-S75, and M-S90 are derived from the optimal distribution by applying a non-linear transformation. Similar to Section IV-C, the efficiency of embedding the antenna deployment within the grid depends on the geometry of the environment and the LoD. Thus, for a fixed LoD, certain geometries allow for a more efficient representation of the optimal transmit antenna deployment than others. Naturally, these fluctuations apply to the suboptimal schemes as well since they are based on the optimal transmit antenna deployment. Specifically, if more grid cells are required for representing the optimal transmit antenna deployment, the respective transmit powers decrease since the overall transmit power remains constant. Consequently, this impacts the number and the position of removed antennas in the suboptimal schemes. The loss in performance compared to the optimal distribution is low for M-S25 and M-S50, which indicates that antennas radiating a relatively low amount of power contribute little to the received power. Therefore, removing these transmit antennas comes at a small loss in received power for the investigated environments. Depending on the geometry of

the environment, M-S75 and M-S90 show a significant loss in receiver power. Especially for low height-to-width ratios, a larger number of transmit antennas operating with lower powers is important for covering the indoor space adequately.

### C. Sensitivity Analysis

In this section, we assess the robustness of the proposed optimal two-dimensional power distribution in the presence of scattering objects in the environment using a Rician fading channel model. The Rician fading channel between transmit antenna  $i$  and the receiver position  $(x, y, z)$  is defined as

$$\tilde{g}_{xz}(a_{ix}, a_{iz}) = \sqrt{\frac{\kappa}{\kappa + 1}} g_{xz}(a_{ix}, a_{iz}) + \sqrt{\frac{1}{\kappa + 1}} h(a_{ix}, a_{iz}), \quad (23)$$

where the constant  $\kappa$  denotes the Rician  $K$ -factor and the LoS channel is given in (6). The NLoS channel vector  $\mathbf{h} = [h(a_{1x}, a_{1z}), \dots, h(a_{(N+1)^2x}, a_{(N+1)^2z})]^T \in \mathbb{C}^{(N+1)^2 \times 1}$  is a realisation of the circularly invariant complex Gaussian distribution  $\mathbf{h} \sim \mathcal{N}_{\mathbb{C}}\left(\mathbf{0}, \frac{c}{\tilde{D}^2} A \mathbf{R}\right)$ , where  $\tilde{D}$  is the average distance between transmitter and receiver [15].  $A$  is the area of a transmit antenna, i.e., the size of a grid element, and the entries of the spatial correlation matrix  $\mathbf{R} \in \mathbb{C}^{(N+1)^2 \times (N+1)^2}$  are given by

$$R_{ij} = \text{sinc}\left(\frac{2}{\lambda} \sqrt{(a_{ix} - a_{jx})^2 + (a_{iz} - a_{jz})^2}\right), \forall i, j = 1, \dots, (N+1)^2, \quad (24)$$

with  $\text{sinc}(x) = \sin(\pi x)/(\pi x)$  [15]. In case of small-scale fading, the propagation environment is no longer deterministic. Consequently, the objective is to maximise the expected value of the received power, i.e.,  $E_H \{\gamma_{xyz}\}$  where  $H$  denotes the random variable describing the Rician fading channel. For the following simulations, the parameters are set to  $\lambda = 3 \cdot 10^{-3}$  m, and  $\kappa = 10$ . All simulations results involving the Rician fading channel were averaged over 100 channel realisations. Moreover, the coefficient of variation (CoV) is provided to indicate the variability of the simulation values in relation to the mean. This dimensionless measure is comparable across the simulation results of different environments.

*1) Discreteness of the optimal solution:* We investigate the sparsity of the transmit antenna deployment at LoD  $N + 1 = 81$  by calculating the number of antennas relative to the number of available grid cells  $(N + 1)^2$ . For the fading environment, the optimal number of transmit antennas was averaged across the channel realisations. The results are given in Tab. II for the LoS environment and the fading environment. For the Rician fading channel, simulations show that the optimal distribution of power is less sparse across all environments compared to the

TABLE II: Percentage of non-zeros in the optimal distribution of power under perfect LoS and in the fading environment at LoD  $N + 1 = 81$ .

$\frac{\text{Height}}{\text{Width}}$	LoS [%]	Rician Mean [%]	Rician CoV [%]
1/1	0.152	0.207	69.029
1/3	0.183	0.688	13.674
1/4	0.198	1.089	11.819
1/5	0.61	1.714	10.102

distribution of power under perfect LoS conditions, i.e., the optimal solution requires a larger number of transmit antennas. Moreover, the CoV is similar across different environments, except for the environment with a height-to-width ratio of 1/1. This system is especially sensitive to channel fluctuations since under LoS conditions, the optimal deployment requires only a single transmit antenna.

2) *Performance comparison:* The performance of the proposed optimal solution in LoS conditions is compared to the one for a small-scale fading environment. The loss in performance is measured by the ratio of the objective value achieved under scattering conditions over the objective value achieved in LoS conditions. Simulations are performed for environments with different geometries and are displayed in Tab. III.

TABLE III: Relative performance to perfect LoS conditions.

$\frac{\text{Height}}{\text{Width}}$	Average Relative Performance [%]	CoV [%]
1/1	91.25	0.1486
1/3	90.89	0.0177
1/4	90.87	0.0196
1/5	90.87	0.013

The performance loss caused by small-scale fading was found to be below 10% throughout the different environments.

## VI. CONCLUSION

In this paper, we proposed an optimisation problem for optimally allocating the transmit power among the radiating elements of a transmit antenna array, which implicitly yielded the optimal transmit antenna deployment. The proposed solution maximises the received powers at

the worst possible receiver positions in an indoor space. This system is especially relevant for environments with a multitude of mobile low-power devices, which require a reliable supply of power, such as wearables. In this scenario, focusing energy beams to every mobile device may not be possible in a reliable manner. Mathematically, the formulated problem bears a resemblance to that of finding the optimal amplitude-constrained input distribution for achieving the information capacity. Consequently, analogous theoretical results are obtained, which guarantee that the optimal transmit antenna positions are spread out within their area of deployment such that they do not form any regions of concentration and do not occupy any measurable area. Furthermore, the optimal number of transmit antennas is shown to be finite for a one-dimensional transmit antenna array. In the environments investigated through simulation, deploying a finite number of antennas is found to be optimal in all cases. Moreover, our proposed method yields a considerable gain compared to benchmark schemes. Additionally, the robustness of the approach has been validated by determining the optimal solution in a fading environment with a strong LoS component. The loss in performance under fading conditions was found to be around 10%. Possible extensions of the proposed approach offer several opportunities for future work. These include the extension of the method to more geometrically challenging environments and more flexible antenna array placements, such as positioning arrays on multiple walls as well as the ceiling of a room.

## APPENDIX A

By definition, any  $P \in \Omega$  is non-negative and bounded by one (see (13)). Observe that given any two distributions  $P_1, P_2 \in \Omega$ , their convex combination  $\lambda P_1 + (1 - \lambda)P_2 \in \Omega$  with coefficient  $\lambda \in [0, 1]$  is a distribution as well. It follows that  $\Omega$  is a convex set [19].

In order to further characterise the set  $\Omega$ , the weak topology on a Hilbert space is defined. A linear functional in  $\Omega$  is a linear map from the Hilbert space to the underlying field. The weak topology on a Hilbert space is defined to be the weakest topology such that all continuous linear functionals on the Hilbert space are continuous [25].

Observe that  $\mathcal{L}^2(\mathcal{X}_a \times \mathcal{Z}_a)$  is an infinite-dimensional vector space equipped with the following inner product [26]

$$\iint_{\mathcal{X}_a \times \mathcal{Z}_a} w(a_x, a_z) v(a_x, a_z) da_x da_z, \quad \forall w(a_x, a_z), v(a_x, a_z) \in \mathcal{L}^2(\mathcal{X}_a \times \mathcal{Z}_a), \quad (25)$$

where  $w(a_x, a_z)$  and  $v(a_x, a_z)$  are arbitrary elements of  $\mathcal{L}^2(\mathcal{X}_a \times \mathcal{Z}_a)$ . This inner product space is complete since completeness is ensured by Lebesgue measurability and Lebesgue integration

[26]. Thus,  $\mathcal{L}^2(\mathcal{X}_a \times \mathcal{Z}_a)$  is a Hilbert space, which is separable since it has a countable orthonormal basis [26]. Note that the set  $\Omega$  is a subset of  $\mathcal{L}^2(\mathcal{X}_a \times \mathcal{Z}_a)$  with bounded elements in  $\Omega$  (see (13)). In a separable Hilbert space, every bounded sequence has a weakly convergent subsequence in the weak topology [25] and therefore,  $\Omega$  is sequentially compact [27]. The concepts of sequential compactness and compactness are equivalent for a separable Hilbert space [25]. Thus,  $\Omega$  is a compact space.

## APPENDIX B

First, Problem (14) is rewritten in epigraph form [19] which yields the following constrained optimisation problem

$$\begin{aligned} & \underset{o \in \mathbb{R}, P \in \Omega}{\text{maximise}} && o \end{aligned} \quad (26a)$$

$$\text{subject to} \quad o \leq \mathbb{E}_P\{f_{xz}\}, \quad \forall (x, y, z) \in \mathcal{X} \times \mathcal{Y}_{\text{crit}} \times \mathcal{Z}, \quad (26b)$$

where  $o$  is bounded by  $m = \min_{(x,y,z) \in \mathcal{X} \times \mathcal{Y}_{\text{crit}} \times \mathcal{Z}} \mathbb{E}_{P^*}\{f_{xz}\}$ . Observe that the objective function and the feasible set of Problem (26) are both affine. Then, if the linear programming problem in (26) admits a solution, i.e., if  $o^* = m$  is finite, duality holds. Furthermore, there exist some  $\lambda_{xz} \geq 0, \forall (x, y, z) \in \mathcal{X} \times \mathcal{Y}_{\text{crit}} \times \mathcal{Z}$  such that the augmented problem

$$\begin{aligned} & \underset{o \in \mathbb{R}, P \in \Omega, \Lambda}{\text{maximise}} && o - \sum_{\mathcal{X} \times \mathcal{Y}_{\text{crit}} \times \mathcal{Z}} (o - \mathbb{E}_P\{f_{xz}\}) \lambda_{xz}, \end{aligned} \quad (27)$$

and Problem (26) are equivalent if the solution  $(o^*, P^*)$  is feasible, i.e., the problem constraints are satisfied in  $(o^*, P^*)$ , and the following complementary slackness conditions hold:

$$\lambda_{xz} (m - \mathbb{E}_{P^*}\{f_{xz}\}) \stackrel{!}{=} 0, \quad \forall (x, y, z) \in \mathcal{X} \times \mathcal{Y}_{\text{crit}} \times \mathcal{Z}. \quad (28)$$

Since  $f_{xz}$  is bounded, the optimal objective value  $o^* = m$  is finite and it is attained in  $P^*$ . The conditions in (28) imply

$$[(\lambda_{xz} > 0 \implies m = \mathbb{E}_{P^*}\{f_{xz}\}) \text{ or } (m < \mathbb{E}_{P^*}\{f_{xz}\} \implies \lambda_{xz} = 0)], \quad \forall (x, y, z) \in \mathcal{X} \times \mathcal{Y}_{\text{crit}} \times \mathcal{Z} \quad (29)$$

From (29), if  $\lambda_{xz} > 0$ , then  $o^* = m = \mathbb{E}_{P^*}\{f_{xz}\}$  and position  $(x, y, z)$  is critical. If  $o^* = m < \mathbb{E}_{P^*}\{f_{xz}\}$ , then  $\lambda_{xz} = 0$  and position  $(x, y, z)$  is non-critical. Thus, the dual variables  $\lambda_{xz}$  are only non-zero for critical receiver locations and it is sufficient to sum over  $\mathcal{R}_{\text{crit}}$  in (27). Thus, under the assumption that  $\mathcal{R}_{\text{crit}}$  is known, the modified augmented problem in (16) along with (29) is equivalent to the augmented problem in (27) together with (29) and thus, to Problem (14).



## APPENDIX C

The continuity of  $E_P\{f_{xz}\}$  in  $P$  is established in the following lemma.

**Lemma C.1.**  $E_P\{f_{xz}\}$  is weakly continuous in the weak topology on a Hilbert space if  $f_{xz}$  is a continuous and bounded function.

*Proof:* Based on Theorem 1 in [22], the linear functional  $E_P\{f_{xz}\}$  is weakly continuous on  $\Omega$  if  $f_{xz}$  is a continuous and bounded function. From Lemma 2,  $f_{xz}$  is a continuous function and bounded since  $y = L_y$ . ■

For the proof of Proposition 1 we apply Theorem 9 in [22]. The convexity and compactness of  $\Omega$  is established in Lemma 1. The continuity of  $J(P)$  is shown in Lemma C.1. The concavity of  $J(P)$  follows from the linearity of  $J(P)$  in  $P$ . Formulating the optimality condition for  $P^*$  requires defining the Gâteaux derivative of  $J(P)$ .

**Definition C.1.** The Gâteaux derivative of the function  $J : \Omega \rightarrow \mathbb{R}$  at  $P$  in the direction of  $Q$  with  $P, Q \in \Omega$  is defined as follows [22]

$$\Delta_Q J(P) = \lim_{\theta \rightarrow 0} \frac{J((1-\theta)P + \theta Q) - J(P)}{\theta}. \quad (30)$$

Moreover, as a linear functional of  $P$ , the Gâteaux derivative of  $J(P)$  in (30) can be expressed as [22]

$$\Delta_Q J(P) = J(Q) - J(P). \quad (31)$$

Theorem 9 in [22] establishes that if  $\Omega$  is a convex set and  $J(P)$  is continuous, concave, and Gâteaux differentiable, then  $J(P)$  attains the maximum value at  $P^* \in \Omega$  if and only if  $\Delta_P J(P^*) \leq 0, \forall P \in \Omega$ . Applying (31) and cancelling the terms that are independent of the distributions  $P$  and  $P^*$ , we obtain

$$\Delta_P J(P^*) = \sum_{\mathcal{R}^{\text{crit}}} \lambda_{xz} E_P\{f_{xz}\} - \sum_{\mathcal{R}^{\text{crit}}} \lambda_{xz} E_{P^*}\{f_{xz}\}. \quad (32)$$

We can further enforce in (32) the constraints on  $\lambda_{xz}$  and  $E_P\{f_{xz}\}$  for the optimal solution  $P^*$  in (17). Then,  $\lambda_{xz}$  is only non-zero for critical receiver locations w.r.t. the optimal distribution  $P^*$ . Furthermore, the objective value for the critical receiver positions is the constant  $E_{P^*}\{f_{xz}\} = m$ . By expanding the expectation operator in (32), the optimality condition  $\Delta_P J(P^*) \leq 0$  can be expressed as

$$\iint_{\mathcal{X}_a \times \mathcal{Z}_a} \frac{\sum_{\mathcal{R}^{\text{crit}}} f_{xz}(a_x, a_z) \lambda_{xz}}{\sum_{\mathcal{R}^{\text{crit}}} \lambda_{xz}} dP(a_x, a_z) = \iint_{\mathcal{X}_a \times \mathcal{Z}_a} \bar{f}(a_x, a_z) dP(a_x, a_z) \leq m, \quad (33)$$

which is satisfied with equality for the optimal distribution of power  $P^*$ .

## APPENDIX D

If the conditions (20) and (21) are satisfied, then conditions (18) and (19) in Proposition 1 are satisfied. In the following, we show that the converse holds as well, i.e., if Proposition 1 holds, then Corollary 1 holds as well. We proceed by contradiction and assume that Proposition 1 holds, however, (20) does not hold. In this case,  $\exists(a_{x1}, a_{z1}) \in \mathcal{X}_a \times \mathcal{Z}_a$ , such that  $\bar{f}(a_{x1}, a_{z1}) > m$ . Suppose,  $(a_{x1}, a_{z1})$  is the only transmit antenna, i.e.,  $(a_{x1}, a_{z1})$  is allocated all the power. Then (18) yields

$$\iint_{\mathcal{X}_a \times \mathcal{Z}_a} \bar{f}(a_x, a_z) dP(a_x, a_z) = \bar{f}(a_{x1}, a_{z1}) > m, \quad (34)$$

which contradicts (18) in Proposition 1. Consequently, if (18) holds, then (20) holds as well.

Next, suppose Proposition 1 holds, however, (21) does not. Define a subset  $\mathcal{E}_0(P^*) \subset \mathcal{E}(P^*)$  such that  $P^*(\mathcal{E}_0(P^*)) = 0$ . Observe that  $\bar{f}(a_x, a_z)$  is continuous on  $\mathbb{R}^2$  since the function's numerator is a weighted sum of continuous functions and the denominator is always a positive constant. Assume there exists a point of increase  $(a_{x1}, a_{z1}) \in \mathcal{E}(P^*) \setminus \mathcal{E}_0(P^*)$  such that  $\bar{f}(a_{x1}, a_{z1}) > m$ . For any  $\delta > 0$  such that  $\bar{f}(a_{x1}, a_{z1}) - \delta > m$ , there exists an open ball  $\mathcal{B}$  centred at  $(a_{x1}, a_{z1})$  such that  $\bar{f}(a_x, a_z) > \bar{f}(a_{x1}, a_{z1}) - \delta > m, \forall (a_x, a_z) \in \mathcal{B}$  which follows from the continuity of  $\bar{f}(a_x, a_z)$ . Since the open ball  $\mathcal{B}$  contains the point of increase  $(a_{x1}, a_{z1}) \in \mathcal{E}(P^*) \setminus \mathcal{E}_0(P^*)$  it follows that  $P^*(\mathcal{B}) > 0$ . This contradicts Proposition 1, i.e.,  $m = \iint_{\mathcal{X}_a \times \mathcal{Z}_a} \bar{f}(a_x, a_z) dP^*(a_x, a_z)$  since

$$\begin{aligned} m &= \underbrace{\iint_{(\mathcal{E}(P^*) \setminus \mathcal{E}_0(P^*)) \cap \mathcal{B}} \bar{f}(a_x, a_z) dP^*(a_x, a_z)}_{> mP^*(\mathcal{B})} + \underbrace{\iint_{(\mathcal{E}(P^*) \setminus \mathcal{E}_0(P^*)) \setminus \mathcal{B}} \bar{f}(a_x, a_z) dP^*(a_x, a_z)}_{= m(1-P^*(\mathcal{B}))} \\ &\quad + \underbrace{\iint_{\mathcal{E}_0(P^*)} \bar{f}(a_x, a_z) dP^*(a_x, a_z)}_{=0} > m. \end{aligned} \quad (35)$$

From this contradiction we have shown that  $\bar{f}(a_x, a_z) = m, \forall (a_x, a_z) \in \mathcal{E}(P^*) \setminus \mathcal{E}_0(P^*)$ . Furthermore, since  $P^*(\mathcal{E}_0(P^*)) = 0$ ,  $\mathcal{E}_0(P^*)$  has no interior points. Any open set of  $\mathbb{R}^2$  containing a point in  $\mathcal{E}_0(P^*)$  intersects points in  $\mathcal{E}(P^*) \setminus \mathcal{E}_0(P^*)$  and therefore, every point in  $\mathcal{E}_0(P^*)$  is in the closure of  $\mathcal{E}(P^*) \setminus \mathcal{E}_0(P^*)$ . Moreover, since  $\bar{f}(a_x, a_z)$  is continuous and bounded, it must also be constant on the closure of  $\mathcal{E}(P^*) \setminus \mathcal{E}_0(P^*)$ . This implies  $\bar{f}(a_x, a_z) = m, \forall (a_x, a_z) \in \mathcal{E}(P^*)$ . Consequently, if (18) holds, then (21) holds as well. Thus, (20) and (21) are necessary and sufficient conditions for  $P^*(a_x, a_z)$ .

## APPENDIX E

The proof is similar to Theorem 12 in [22].

The characterisation of the set of optimal transmit antenna positions requires the introduction of the following definitions. A subset  $S_1 \subset S_0$  is *dense* in  $S_0$  if every element  $s \in S_0$  is either an element of  $S_1$  or an accumulation point of  $S_1$  [22]. A subset  $S_1 \subset S_0$  is *nowhere dense* if  $S_2 \cap S_1$  is not *dense* in  $S_0$ , where  $S_2$  is any non-empty open set  $S_2 \subset S_0$  [22]. Moreover, the characterisation of the support  $\mathcal{E}$  requires the Identity Theorem for real-analytic functions, which is stated, e.g., in [28]. The Identity Theorem states that if two real-analytic functions  $f_1$  and  $f_2$ , which are defined on an open set  $U \subseteq \mathbb{R}^n$ , take the same value on an open subset  $W \subseteq U$ , i.e.,  $f_1(w) = f_2(w), \forall w \in W$ , then  $f_1(u) = f_2(u), \forall u \in U$ .

Next, we show that  $\bar{f}(a_x, a_z)$  is not constant in  $\mathcal{X}_a \times \mathcal{Z}_a$ . Thereby, it suffices to show that the partial derivative of  $\bar{f}(a_x, a_z)$  w.r.t.  $a_x$ , with  $a_z = 0$ , is not zero  $\forall (a_x, a_z) \in \mathcal{X}_a \times \mathcal{Z}_a$ . Note that

$$\frac{\partial \bar{f}(a_x, a_z)}{\partial a_x} = \frac{\sum_{\mathcal{R}_{\text{crit}}} \frac{2(x - a_x)}{((z - a_z)^2 + (x - a_x)^2 + L_y^2)^2} \lambda_{xz}}{\sum_{\mathcal{R}_{\text{crit}}} \lambda_{xz}}, \quad (36)$$

is only zero for  $x = a_x$  and non-zero otherwise. Consequently,  $\bar{f}(a_x, a_z)$  is not constant in  $\mathcal{X}_a \times \mathcal{Z}_a$ .

Next, we show that  $\bar{f}(a_x, a_z)$  is real-analytic in  $\mathbb{R}^2$  and thus, in  $\mathcal{X}_a \times \mathcal{Z}_a$ . Let  $\bar{f}(a_x, a_z) = kn(a_x, a_z)$ , where  $k = (\sum_{\mathcal{R}_{\text{crit}}} \lambda_{xz})^{-1}$  is a positive constant for all  $(a_x, a_z)$  and  $n(a_x, a_z) = \sum_{\mathcal{R}_{\text{crit}}} f_{xz}(a_x, a_z) \lambda_{xz}$ . The function  $\bar{f}(a_x, a_z)$  is real-analytic in  $(a_x, a_z)$  if  $n(a_x, a_z)$  is an analytic function. The function  $n(a_x, a_z)$  is real-analytic in  $(a_x, a_z)$  if  $f_{xz}(a_x, a_z) \lambda_{xz}$  is real-analytic for fixed  $(x, z)$ . Thereby, it suffices to show that  $f_{xz}(a_x, a_z)$  is real-analytic since  $\lambda_{xz}$  is some non-negative constant scaling  $f_{xz}(a_x, a_z)$ .

Note that the composition of real-analytic functions is real-analytic [28]. By rewriting  $f_{xz}(a_x, a_z)$  as  $f(w_{xz}(a_x, a_z)) = 1/(L_y^2 + w_{xz}(a_x, a_z))$ , where  $w_{xz}(a_x, a_z) = (x - a_x)^2 + (z - a_z)^2 \geq 0$ , it is sufficient to show that both  $w_{xz}(a_x, a_z)$  and  $f(w) = 1/(w + L_y^2) > 0$  are real-analytic. By definition, polynomials are real-analytic functions [28], thus  $w_{xz}(a_x, a_z)$  is real-analytic. Next, the real function  $f(w)$  is shown to be analytic by proving that it's complex extension  $f(r_1 + jr_2) = u(r_1, r_2) + jv(r_1, r_2) = (r_1 + L_y^2)/((r_1 + L_y)^2 + r_2^2) - jr_2/((r_1 + L_y)^2 + r_2^2)$  is holomorphic. Function  $f(w)$  is holomorphic and thus, analytic, if it satisfies the Cauchy-Riemann (CR) equations [29]. The CR equations are given by [29]

$$\frac{\partial u(r_1, r_2)}{\partial r_1} = \frac{\partial v(r_1, r_2)}{\partial r_2}, \quad (37)$$

$$\frac{\partial u(r_1, r_2)}{\partial r_2} = -\frac{\partial v(r_1, r_2)}{\partial r_1}, \quad (38)$$

Clearly, the CR equations are satisfied for the complex extension  $f(r_1 + jr_2)$  since

$$\frac{\partial u(r_1, r_2)}{\partial r_1} = \frac{\partial v(r_1, r_2)}{\partial r_2} = \frac{r_2^2 - (L_y^2 + r_1)^2}{((L_y^2 + r_1)^2 + r_2^2)^2}, \quad (39)$$

$$\frac{\partial u(r_1, r_2)}{\partial r_2} = -\frac{\partial v(r_1, r_2)}{\partial r_1} = \frac{-2r_2(L_y^2 + r_1)}{((L_y^2 + r_1)^2 + r_2^2)^2}, \quad (40)$$

which proves that the complex extension  $f(r_1 + jr_2)$  is analytic. Consequently,  $\bar{f}(a_x, a_z)$  is real-analytic in  $\forall(a_x, a_z) \in \mathbb{R}^2$  and thus, in  $\forall(a_x, a_z) \in \mathcal{X}_a \times \mathcal{Z}_a$ .

Suppose that  $\mathcal{E}(P^*)$  is not a nowhere dense set in  $\mathcal{X}_a \times \mathcal{Z}_a$ . Consequently, there exists some non-empty open set  $\mathcal{E}_2 \subset \mathcal{X}_a \times \mathcal{Z}_a$  such that  $\mathcal{E}_2 \cap \mathcal{E}(P^*)$  is dense in  $\mathcal{X}_a \times \mathcal{Z}_a$ . From (21),  $\bar{f}(a_x, a_z) = m$  is constant on  $\mathcal{E}(P^*)$  and thus, constant on  $\mathcal{E}_2 \cap \mathcal{E}(P^*)$ . Since  $\bar{f}(a_x, a_z)$  is real-analytic, the Identity Theorem of real-analytic functions applies and thus,  $\bar{f}(a_x, a_z)$  must be constant on  $\mathcal{X}_a \times \mathcal{Z}_a$ . However,  $\bar{f}(a_x, a_z) \neq \text{const.}, \forall(a_x, a_z) \in \mathcal{X}_a \times \mathcal{Z}_a$ . From this contradiction,  $\mathcal{E}(P^*) \subset \mathcal{X}_a \times \mathcal{Z}_a$  must be a nowhere dense set of  $\mathcal{X}_a \times \mathcal{Z}_a$ .

## APPENDIX F

Suppose  $\mathcal{E}(P^*)$  is of positive Lebesgue measure. For any open subset  $\mathcal{V} \subset \mathcal{E}(P^*)$ , the function  $\bar{f}(a_x, a_z)$  is constant on  $\mathcal{V}$  since it is constant on  $\mathcal{E}(P^*)$ . Since  $\bar{f}(a_x, a_z)$  is real-analytic as shown in Appendix E, the Identity Theorem, e.g., [28] of real-analytic functions applies and thus,  $\bar{f}(a_x, a_z)$  must be constant on  $\mathcal{X}_a \times \mathcal{Z}_a$ . However, as shown in Appendix E,  $\bar{f}(a_x, a_z) \neq \text{const.}, \forall(a_x, a_z) \in \mathcal{X}_a \times \mathcal{Z}_a$ . From this contradiction,  $\mathcal{E}(P^*) \subset \mathcal{X}_a \times \mathcal{Z}_a$  must have Lebesgue measure zero.

## APPENDIX G

The proof is also analogous to [20], [21].

This proof requires the application of the Bolzano-Weierstrass theorem which states that in the set of real numbers any infinite bounded sequence of real numbers has a convergent subsequence and the limit of that subsequence is an accumulation point of the original sequence [30]. In the following  $\bar{f}(a_l)$  is a function defined over a one-dimensional set, i.e.,  $\bar{f} : \mathcal{L}_a \rightarrow \mathbb{R}$ , with  $\mathcal{L}_a \subset \mathcal{X}_a \times \mathcal{Z}_a$  and  $\tilde{\mathcal{E}}(\tilde{P}^*)$  is the optimal set of transmit antenna positions, which is bounded, i.e.,  $\tilde{\mathcal{E}}(\tilde{P}^*) \subset \mathcal{L}_a$ . Suppose the set  $\tilde{\mathcal{E}}(\tilde{P}^*)$  is not finite. From the Bolzano-Weierstrass theorem, it follows that  $\tilde{\mathcal{E}}(\tilde{P}^*)$  has an accumulation point  $q$ . Based on (21), define the function  $s(a_l) =$

$m - \bar{f}(a_l)$ , which is equal to zero  $\forall a_l \in \tilde{\mathcal{E}}$ . Moreover,  $s(a_l)$  is analytic since it is the sum of analytic functions [28]. By assuming  $\tilde{\mathcal{E}}(\tilde{P}^*)$  is not finite,  $s$  has infinitely many zeros. Moreover, the accumulation point  $q$  is also a zero of function  $s(a_l)$ , i.e.,  $s(q) = 0$ , since  $s(a_l)$  is a continuous function, which is implied by the analyticity of  $s(a_l)$ . Then from the Identity Theorem, e.g. [28],  $s(a_l)$  coincides with zero in the entire set  $\mathcal{L}_a$  or equivalently

$$\bar{f}(a_l) = m, \forall a_l \in \mathcal{L}_a, \quad (41)$$

which implies that  $\bar{f}$  is constant on  $\mathcal{L}_a$ . However,  $\bar{f}$  is not constant on  $\mathcal{L}_a$  as shown in Appendix E. Consequently,  $\tilde{\mathcal{E}}(\tilde{P}^*)$  must be a finite set.

## REFERENCES

- [1] H. Rahmani, D. Shetty, M. Wagih, Y. Ghasempour, V. Palazzi, N. B. Carvalho, R. Correia, A. Costanzo, D. Vital, F. Alimenti, J. Kettle, D. Masotti, P. Mezzanotte, L. Roselli, and J. Grosinger, "Next-Generation IoT Devices: Sustainable Eco-Friendly Manufacturing, Energy Harvesting, and Wireless Connectivity," *IEEE J. Microwaves*, vol. 3, no. 1, pp. 237–255, Jan. 2023.
- [2] F. John Dian, R. Vahidnia, and A. Rahmati, "Wearables and the Internet of Things (IoT), Applications, Opportunities, and Challenges: A Survey," *IEEE Access*, vol. 8, Apr. 2020.
- [3] D. Verma, K. R. Singh, A. K. Yadav, V. Nayak, J. Singh, P. R. Solanki, and R. P. Singh, "Internet of things (IoT) in Nano-Integrated Wearable Biosensor Devices For Healthcare Applications," *Biosens. Bioelectron.*: X, vol. 11, Sep. 2022.
- [4] D. Metcalf, S. T. Milliard, M. Gomez, and M. Schwartz, "Wearables and the Internet of Things for Health: Wearable, Interconnected Devices Promise More Efficient and Comprehensive Health Care," *IEEE Pulse*, vol. 7, no. 5, Sept.-Oct. 2016.
- [5] M. Wagih, L. Balocchi, F. Benassi, N. B. Carvalho, J.-C. Chiao, R. Correia, A. Costanzo, Y. Cui, D. Georgiadou, C. Gouveia, J. Grosinger, J. S. Ho, K. Hu, A. Komolafe, S. Lemey, C. Loss, G. Marrocco, P. Mitcheson, V. Palazzi, N. Panunzio, G. Paolini, P. Pinho, J. Preishuber-Pflügl, Y. Qaragoz, H. Rahmani, H. Rogier, J. R. Lopera, L. Roselli, D. Schreurs, M. Tentzeris, X. Tian, R. Torah, R. Torres, P. Van Torre, D. Vital, and S. Beeby, "Microwave-enabled wearables: Underpinning technologies, integration platforms, and next-generation roadmap," *IEEE J. Microwaves*, vol. 3, no. 1, pp. 193–226, Jan. 2023.
- [6] M. Wagih, A. S. Weddell, and S. Beeby, "Millimeter-wave power harvesting: A review," *IEEE Open J. Antennas Propag.*, vol. 1, pp. 560–578, Dec. 2020.
- [7] H. Zhang, N. Shlezinger, F. Guidi, D. Dardari, M. F. Imani, and Y. C. Eldar, "Near-Field Wireless Power Transfer for 6G Internet of Everything Mobile Networks: Opportunities and Challenges," *IEEE Commun. Mag.*, vol. 60, no. 3, Mar. 2022.
- [8] H. Zhang, N. Shlezinger, F. Guidi, D. Dardari, and Y. C. Eldar, "6G Wireless Communications: From Far-Field Beam Steering to Near-Field Beam Focusing," *IEEE Commun. Mag.*, vol. 61, no. 4, Apr. 2023.
- [9] S. Hu, F. Rusek, and O. Edfors, "Beyond Massive MIMO: The Potential of Data Transmission with Large Intelligent Surfaces," *IEEE Trans. Signal Process.*, vol. 66, no. 10, pp. 2746–2758, May 2018.
- [10] D. Dardari and N. Decarli, "Holographic Communication Using Intelligent Surfaces," *IEEE Commun. Mag.*, vol. 59, no. 6, pp. 35–41, June 2021.
- [11] H. Zhang, N. Shlezinger, F. Guidi, D. Dardari, M. F. Imani, and Y. C. Eldar, "Beam Focusing for Near-Field Multiuser MIMO Communications," *IEEE Trans. Wirel. Commun.*, vol. 21, no. 9, pp. 7476–7490, Sep. 2022.
- [12] H. Do, S. Cho, J. Park, H.-J. Song, N. Lee, and A. Lozano, "Terahertz Line-of-Sight MIMO Communication: Theory and Practical Challenges," *IEEE Commun. Mag.*, vol. 59, no. 3, pp. 104–109, Mar. 2021.

- [13] X. Li, H. Lu, Y. Zeng, S. Jin, and R. Zhang, “Near-Field Modelling and Performance Analysis of Modular Extremely Large-Scale Array Communications,” *IEEE Commun. Lett.*, pp. 1–5, Jul. 2022.
- [14] D. Tse and P. Viswanath, *Fundamentals of Wireless Communication*. Cambridge, UK: Cambridge University Press, 2005.
- [15] E. Björnson and L. Sanguinetti, “Rayleigh Fading Modeling and Channel Hardening for Reconfigurable Intelligent Surfaces,” *IEEE Wirel. Commun. Lett.*, vol. 10, no. 4, pp. 830–834, Apr. 2021.
- [16] A. Pizzo, T. L. Marzetta, and L. Sanguinetti, “Spatially-Stationary Model for Holographic MIMO Small-Scale Fading,” *IEEE J. Sel. Areas Commun.*, vol. 38, no. 9, pp. 1964–1979, Sept. 2020.
- [17] E. Björnson, J. Hoydis, and L. Sanguinetti, “Massive MIMO Networks: Spectral, Energy, and Hardware Efficiency,” *Found. Trends Signal Process.*, vol. 11, no. 3–4, pp. 154–655, 2017. [Online]. Available: <http://dx.doi.org/10.1561/20000000093>
- [18] B. Clerckx, J. Kim, K. W. Choi, and D. I. Kim, “Foundations of wireless information and power transfer: Theory, prototypes, and experiments,” *Proc. IEEE*, vol. 110, no. 1, pp. 8–30, Jan. 2022.
- [19] S. P. Boyd and L. Vandenberghe, *Convex Optimization*. Cambridge, UK: Cambridge University Press, 2004.
- [20] J. G. Smith, “The Information Capacity of Amplitude- and Variance-Constrained Scalar Gaussian Channels,” *Inf. Control.*, vol. 18, no. 3, pp. 203–219, Apr. 1971.
- [21] R. Morsi, V. Jamali, A. Hagelauer, D. W. K. Ng, and R. Schober, “Conditional Capacity and Transmit Signal Design for SWIPT Systems with Multiple Nonlinear Energy Harvesting Receivers,” *IEEE Trans. Commun.*, vol. 68, no. 1, pp. 582–601, Jan. 2020.
- [22] A. Dytso, M. Goldenbaum, H. V. Poor, and S. S. Shitz, “When are discrete channel inputs optimal? — Optimization techniques and some new results,” in *52nd Annu. Conf. Inf. Sci. Syst.*, 2018, pp. 1–6.
- [23] S. Diamond and S. Boyd, “CVXPY: A Python-Embedded Modeling Language for Convex Optimization,” *J. Mach. Learn. Res.*, vol. 17, no. 83, pp. 1–5, Mar. 2016.
- [24] A. Agrawal, R. Verschueren, S. Diamond, and S. Boyd, “A Rewriting System for Convex Optimization Problems,” *J. Control Decis.*, vol. 5, no. 1, pp. 42–60, Jan. 2018.
- [25] W. Rudin, *Functional Analysis*. McGraw Hill, 1991.
- [26] M. Vetterli, J. Kovačević, and V. K. Goyal, *Foundations of Signal Processing*. Cambridge, UK: Cambridge University Press, 2014.
- [27] S. Willard, *General Topology*. Dover Publications, 2004.
- [28] S. G. Krantz and H. R. Parks, *A Primer of Real Analytic Functions*. Springer, 2002.
- [29] W. Rudin, *Real and Complex Analysis*. McGraw Hill, 1987.
- [30] —, *Principles of Mathematical Analysis*. McGraw Hill, 1976.